

Basic Study

Asiaticoside improves diabetic nephropathy by reducing inflammation, oxidative stress, and fibrosis: An *in vitro* and *in vivo* study

Lan-Gen Zhuang, Rong Zhang, Guo-Xi Jin, Xiao-Yan Pei, Qiong Wang, Xiao-Xu Ge

Specialty type: Endocrinology and metabolism**Provenance and peer review:** Unsolicited article; Externally peer reviewed.**Peer-review model:** Single blind**Peer-review report's classification****Scientific Quality:** Grade A, Grade B, Grade C, Grade C**Novelty:** Grade A, Grade B**Creativity or Innovation:** Grade A, Grade B**Scientific Significance:** Grade A, Grade A**P-Reviewer:** Dabla PK; Islam MS; Mohammadi S**Received:** March 7, 2024**Revised:** May 30, 2024**Accepted:** July 22, 2024**Published online:** October 15, 2024**Processing time:** 202 Days and 18.2 Hours**Lan-Gen Zhuang, Guo-Xi Jin, Xiao-Yan Pei, Qiong Wang,** Department of Endocrinology, The First Affiliated Hospital of Bengbu Medical College, Bengbu 233004, Anhui Province, China**Rong Zhang,** Department of Nephrology, Shanghai General Hospital, Shanghai Jiao Tong University School of Medicine, Shanghai 200025, China**Xiao-Xu Ge,** Department of Endocrinology, Tongren Hospital Affiliated to Shanghai Jiao Tong University, Shanghai 200336, China**Corresponding author:** Xiao-Xu Ge, MD, Doctor, Department of Endocrinology, Tongren Hospital Affiliated to Shanghai Jiao Tong University, No. 1111 Xianxia Road, Changning District, Shanghai 200336, China. uyhyt41964@163.com**Abstract****BACKGROUND**

Diabetic nephropathy (DN) is a severe microvascular complication of diabetes characterized by inflammation, oxidative stress, and renal fibrosis. Asiaticoside (AC) exhibits anti-inflammatory, antioxidant, and anti-fibrotic properties, suggesting potential therapeutic benefits for DN. This study aimed to investigate the protective effects of AC against DN and elucidate the underlying mechanisms involving the nuclear factor erythroid 2-related factor 2 (NRF2)/heme oxygenase-1 (HO-1) antioxidant pathway.

AIM

To investigate the renoprotective effects of AC against DN and elucidate the role of the NRF2/HO-1 pathway.

METHODS

The effects of AC on high glucose (HG)-induced proliferation, inflammation, oxidative stress, and fibrosis were evaluated in rat glomerular mesangial cells (HBZY-1) *in vitro*. A streptozotocin-induced DN rat model was established to assess the *in vivo* impact of AC on renal injury, inflammation, oxidative stress, and fibrosis. The involvement of the NRF2/HO-1 pathway was examined using pharmacological inhibition studies in the cell model.

RESULTS

AC inhibited HG-induced HBZY-1 cell proliferation and significantly improved various indicators of DN in rats, including reduced body weight, and elevated blood glucose, serum creatinine, blood urea nitrogen, and 24-h urine protein. Both *in vitro* and *in vivo* studies demonstrated that AC decreased inflammation and oxidative stress by reducing interleukin (IL)-6, IL-8, tumor necrosis factor- α , reactive oxygen species, and malondialdehyde levels while increasing superoxide dismutase activity. Additionally, AC suppressed the expression of fibrogenic markers such as collagen I, collagen IV, and fibronectin. AC activated NRF2 expression in the nucleus and increased HO-1 and NAD(P)H dehydrogenase (Quinone) 1 protein expression in renal tissues and HG-induced HBZY-1 cells.

CONCLUSION

AC improves DN by reducing inflammation, oxidative stress, and fibrosis through the activation of the NRF2/HO-1 signaling pathway. These findings not only highlight AC as a promising therapeutic candidate for DN but also underscore the potential of targeting the NRF2/HO-1 pathway in developing novel treatments for other chronic kidney diseases characterized by oxidative stress and inflammation.

Key Words: Asiaticoside; Diabetic nephropathy; Inflammation; Renal fibrosis; Reactive oxygen species

©The Author(s) 2024. Published by Baishideng Publishing Group Inc. All rights reserved.

Core Tip: This study investigated the protective effects of asiaticoside (AC) in diabetic nephropathy (DN) using *in vitro* and *in vivo* models. AC attenuated high glucose-induced proliferation, inflammation, oxidative stress, and fibrosis in rat glomerular mesangial cells. In a streptozotocin-induced DN rat model, AC ameliorated renal injury, and reduced inflammatory cytokines, oxidative stress markers, and fibrogenic markers. Notably, the renoprotective effects of AC were associated with the activation of the nuclear factor erythroid 2-related factor 2 (NRF2)/heme oxygenase-1 antioxidant signaling pathway, suggesting AC's therapeutic potential for DN by targeting inflammation, oxidative stress, and fibrosis through NRF2-associated mechanisms.

Citation: Zhuang LG, Zhang R, Jin GX, Pei XY, Wang Q, Ge XX. Asiaticoside improves diabetic nephropathy by reducing inflammation, oxidative stress, and fibrosis: An *in vitro* and *in vivo* study. *World J Diabetes* 2024; 15(10): 2111-2122

URL: <https://www.wjgnet.com/1948-9358/full/v15/i10/2111.htm>

DOI: <https://dx.doi.org/10.4239/wjd.v15.i10.2111>

INTRODUCTION

Diabetic nephropathy (DN), a severe microvascular complication of diabetes mellitus, is known for its low cure rate, low awareness rate, high morbidity, and high disability[1,2]. In the advanced stages of diabetes, DN transitions from mild renal inflammation to various phases of renal fibrosis, renal sclerosis, and ultimately end-stage renal disease (ESRD)[3]. Studies have shown that after 20 years of diabetes, the prevalence of DN could be as high as 30%-40%, with 5%-10% of patients progressing to ESRD. Projections suggest that DN may become the seventh leading cause of death worldwide by 2030[3-6]. While strict control of blood glucose levels and blood pressure is crucial in managing DN, some cases still progress to ESRD despite successful glucose control. Therefore, the development of new therapeutic modalities and drugs for DN is essential.

Before delving into therapeutic options, it is crucial to elucidate the complex pathogenesis of DN, which remains incompletely understood. Recent research efforts have suggested that hyperglycemia-induced oxidative stress may be a key factor in the development of renal complications in diabetes. Moreover, inflammation in renal tissues plays a vital role in the onset and progression of DN[7]. Oxidative stress typically arises from an overproduction of reactive oxygen species (ROS) or a decrease in antioxidant capacity. In diabetes, elevated ROS levels can disrupt the intracellular metabolism of DNA, proteins, and lipids through oxidative modifications, leading to renal dysfunction by activating various cellular signaling pathways[8,9]. The combination of hyperglycemia and excessive intracellular ROS can trigger renal cells to produce cytokines such as tumor necrosis factor (TNF)- α and interleukin (IL)-6. These ROS and cytokines then interact, leading to the activation of inflammatory factors, adhesion molecules, and chemokines. The resulting inflammation contributes to glomerulosclerosis and tubulointerstitial fibrosis, which exacerbates renal damage and promotes DN progression. Therefore, reducing oxidative stress and mitigating inflammatory damages could be a beneficial therapeutic approach for managing DN.

Nuclear factor erythroid 2-related factor 2 (NRF2), a protein linked to oxidative stress, plays a significant role in DN inflammation. Evidence suggests the implication of NRF2 in DN progression, as it has been shown to regulate pro-inflammatory cytokine production, reduce inflammation, and counteract oxidative stress for renal protection[10]. NRF2 associates with Kelch-like ECH-associated protein 1 in the cytoplasm. When triggered by external factors, it translocates to the nucleus to bind to antioxidant response elements in the promoters of genes like heme oxygenase-1 (HO-1) and

NAD(P)H dehydrogenase (Quinone) 1 (NQO-1). This leads to augmented antioxidant capacity, aiding in the fight against oxidative stress[11].

Asiaticoside (AC), a primary compound of ursane-type triterpene glycoside derived from *Centella asiatica*, has a history of over 2000 years in traditional Chinese medicine for treating a variety of ailments. Multiple studies have shown that AC exhibits antioxidant, anti-inflammatory, anti-fibrotic, and other important pharmacological properties[12-14]. Additionally, AC has been found to activate NRF2 and suppress ROS production, making it a potent compound to boost antioxidant capacity[15]. The current study aimed to investigate the protective effects of AC against inflammation, oxidative stress, and fibrosis in a rat model of DN and high-glucose (HG) induced glomerular mesangial cells, and elucidate the potential underlying mechanisms involving the Nrf2/HO-1 antioxidant pathway. The impact of AC on HG induced proliferation of rat mesangial cells (HBZY-1) was initially examined. Furthermore, we established a streptozotocin (STZ)-induced DN rat model to evaluate the *in vivo* effects of AC on renal injury, inflammation, oxidative stress, and fibrosis. The role of the NRF2/HO-1 pathway in mediating the protective effects of AC was also explored using pharmacological inhibition of NRF2. The findings from this study will provide insights into the therapeutic potential of AC for DN and elucidate a possible mechanism involving the activation of the NRF2 antioxidant pathway.

MATERIALS AND METHODS

Cells and culture conditions

The rat mesangial cell line HBZY-1 was procured from Wuhan Boster Biotechnology Company in Wuhan, China. HBZY-1 cells were cultured in Dulbecco's Modified Eagle Medium (DMEM) from HyClone Laboratories Ltd. in Logan, United States, supplemented with 10% fetal bovine serum from Sangon Biotech in Shanghai, China, 100 µg/mL streptomycin, and 100 U/mL penicillin from HyClone, and maintained under specified conditions (50 mL/L CO₂ and 37 °C). The stock solution of AC (C₄₈H₇₈O₁₉; CAS: 16830-15-2; Figure 1A) was obtained from Yuan Ye Biotechnology Co. Ltd. in Shanghai, China. This solution was prepared by dissolving 95.90 mg of AC in 100 mL of dimethyl sulfoxide from Santa Cruz Biotechnology. Subsequently, the full culture medium was used to create a working solution of varying concentrations.

Cell Counting Kit assay

HBZY-1 cells in the logarithmic growth phase were harvested and plated at a density of 1 × 10⁴ cells/well in 96-well plates for overnight incubation to ensure proper attachment. Subsequently, the cells were exposed to various treatments using AC solutions at different concentrations (0, 0.5, 1.0, 2.0, 4.0, 8.0, 16.0, and 32.0 mmol/L), or with AC solutions (0, 2, 4, and 8 mmol/L) in combination with glucose (5.5 mmol/L), mannitol (30.0 mmol/L), and HG (30.0 mmol/L). After 24 h, each well was supplemented with 10% Cell Counting Kit-8 (CCK-8) working reagent (CA1210, Beijing Solebo Science and Technology Co. Ltd., Beijing, China), followed by incubation at 37 °C for 2 h. Finally, the absorbance values were determined at a wavelength of 450 nm using a microplate reader. For cytotoxicity assay, cells were treated with AC or HG for 24 h, and cells were subjected to indicated treatment for 48 h in cell proliferation assay.

Animal model and treatment options

Male Sprague-Dawley rats (*n* = 40, 8-week-old) were purchased from Shanghai SLAC Laboratory Animal Co. All experimental protocols were approved by the Institutional Animal Ethics Committee of Bengbu Medical College (2022-117). The rats were randomly assigned to different treatment groups including control, DN model, AC drug, and DN + AC. A rat model was established based on a previously published study[16], which is a commonly used animal model for diabetes induction and the study of DN progression. Rats in the DN and DN + AC groups were given a high-fat diet for 8 wk, while those of the control and AC drug groups were given a normal diet. At week 5, these rats were injected intraperitoneally with 60 mg/kg of STZ (v900890-1 g; Sigma, St. Louis, MO, United States), while rats in the control and AC drug groups received normal saline injections. Changes in body weight, blood glucose, kidney weight/body weight ratio (mg/g), serum creatinine, blood urea nitrogen, and 24-h urine protein, as well as histological changes, were analyzed to confirm the onset of DN. After DN induction, rats in the AC and DN + AC groups were administered with AC (dissolved in normal saline) at 10 mg/kg body weight/d by gavage for 4 wk, while the DN and control groups were administered the same volume of normal saline alone.

Renal histology and electron microscopy

The samples for the renal histological studies were prepared following a specific protocol. The animals were euthanized by cervical dislocation. Following euthanasia, the right kidney of each rat was immediately dissected and fixed with 40 g/L paraformaldehyde at room temperature for over 24 h. Subsequently, the samples underwent standard histological analysis procedures and were stained with hematoxylin and eosin (H&E), Masson's, and Periodic acid-Schiff (PAS) stains. The stained tissue sections were then examined using confocal laser scanning microscopy for analysis. Additionally, to observe ultrastructural changes in the kidney, the prepared samples underwent transmission electron microscopy (TEM) following standard procedures. The resulting TEM images were recorded and analyzed.

Quantitative real-time polymerase chain reaction analysis

Total RNA was extracted from digested HBZY-1 cells using Trizol reagent (Invitrogen, Carlsbad, CA, United States). Subsequently, cDNA was synthesized from 2 µg of total RNA with a cDNA synthesis kit (Takara Co. Ltd., Dalian, China). The quantitative real-time polymerase chain reaction (qRT-PCR) analysis was carried out using the SYBR Premix Ex

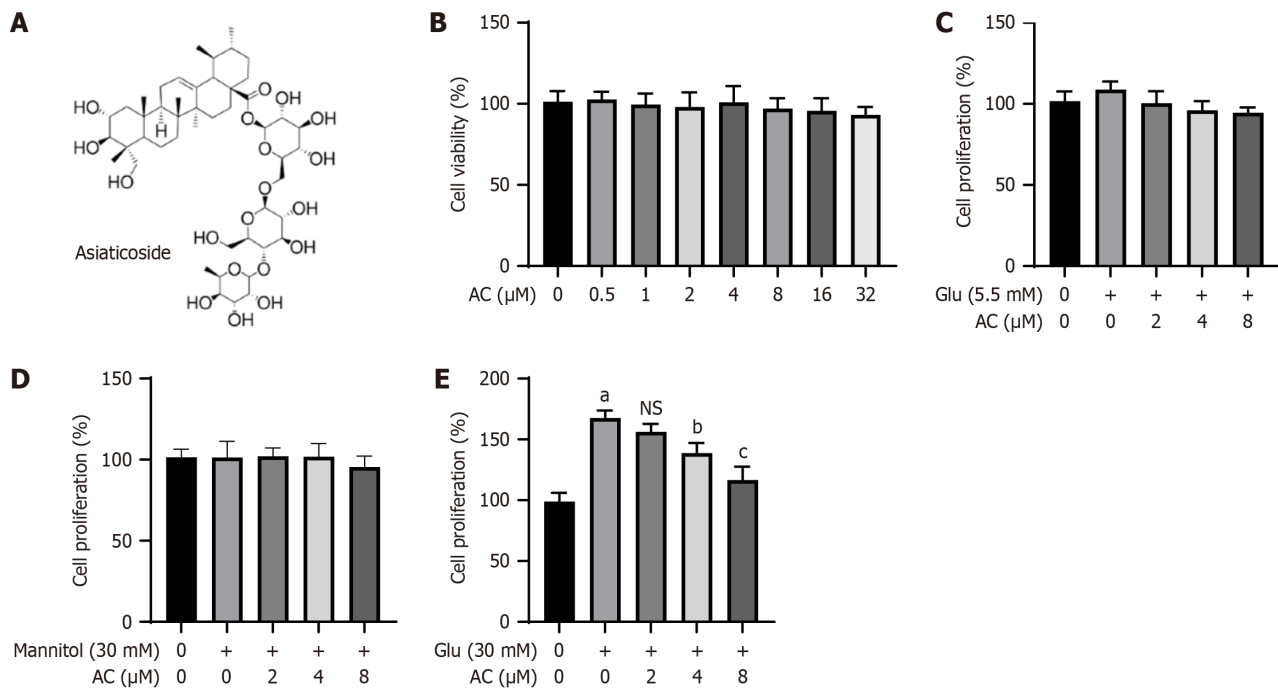


Figure 1 Effect of asiaticoside on high glucose-induced proliferation of rat glomerular mesangial cells. A: Chemical structure of asiaticoside (AC); B: Viability of rat glomerular mesangial cells (HBZY-1) treated with AC at different concentrations (0, 0.5, 1.0, 2.0, 4.0, 8.0, 16.0, and 32.0 μM) for 24 h detected by Cell Counting Kit-8 (CCK-8) assay; C: Proliferation levels of HBZY-1 cells after co-treatment of AC at different concentrations (0, 2, 4, and 8 μM) and glucose (5.5 mmol/L) for 48 h detected by CCK-8 assay; D: Proliferation of HBZY-1 cells after co-treatment of AC treatment at different concentrations (0, 2, 4, and 8 μM) and mannitol (30 mmol/L) detected by CCK-8 assay; E: Proliferation of HBZY-1 cells treated with AC at different concentrations (0, 2, 4, and 8 μM) and glucose (30 mmol/L) detected by CCK-8 assay. *n* = 3 experiments. ^a*P* < 0.001 vs control, ^b*P* < 0.01, and ^c*P* < 0.001 vs (Glu, 30 mmol/L + AC, 0 μM); not significant (*P* > 0.05) vs (Glu, 30 mmol/L + AC 0 μM). AC: Asiaticoside; Glu: Glucose; NS: Not significant.

TAQTM II kit (Takara) to measure *IL-6*, *IL-8*, *TNF-α*, and collagen I levels in HBZY-1 cells from different groups (Con, HG, HG + 2 μM of AC, HG + 4 μM of AC, and HG + 8 μM of AC), along with mRNA levels of collagen IV and fibronectin. Finally, the relative fold change in gene expression was determined using the 2^{-ΔΔCt} method.

The sequences for the forward (F) and reverse (R) primers are as follows: *IL-6*: F, 5'-CCAGTTGCCTTCTTGGGACT-3' and R, 5'-TCTGACAGTGCATCATCGCT-3'; *IL-8*: F, 5'-GAGTTTGAAGGTGATGCCGC-3' and R, 5'-CTTCTGAACCATGGGGCTT-3'; *TNF-α*: F, 5'-ACTGAACCTCGGGGIGATCG-3' and R, 5'-GCTTGGTGGTTTGTCTACGAC-3'; Collagen I: F, 5'-ACATGTTTCAGCTTTGTGGACC-3' and R, 5'-CTTTGCATAGCACGCCATCG-3'; Collagen IV: F, 5'-GCCCCGTG-GATCCCATAGGT-3' and R, 5'-GGAGCAGCAACAGGATAGGC-3'; Fibronectin: F, 5'-GGATCCCCCTCCAGAGAAGT-3' and R, 5'-GGGTGTGGAAGGGTAACCAG-3'; and *GAPDH*: F, 5'-CCGCATCTTCTTGTGCAGTG-3' and R, 5'-ACCAGCTTCCATTCTCAGC-3'

Enzyme-linked immunosorbent assay

The enzyme-linked immunosorbent assay (ELISA) tests were conducted using corresponding kits *as per* the standard procedure. Initially, the medium from the treated HBZY-1 cells was collected and centrifuged at 13000 × *g* for 10 min. Subsequently, the levels of *IL-6*, *IL-8*, and *TNF-α* in the isolated cell supernatants were determined using commercial ELISA Kits from Jikai Biotechnology, Shanghai, China, following the instructions provided by the manufacturer.

Redox state assessment

The redox state was assessed by quantifying the levels of malondialdehyde (MDA), superoxide dismutase (SOD), and ROS. Specifically, MDA content, SOD activity, and ROS content in HBZY-1 cells or tissues were measured with an MDA assay kit (Nanjing Jiancheng Institute of Biological Engineering), total SOD activity assay kit (Nanjing Jiancheng Institute of Biological Engineering), and ROS assay kit (Beijing Solebo Technology Co. Ltd.), respectively, following the provided instructions.

Western blot analysis

HBZY-1 cells or renal tissues were subjected to lysis using Radio Immunoprecipitation Assay (RIPA) buffer containing protease inhibitor (Beyotime, Shanghai, China). Protein concentrations were determined with the bicinchoninic acid Protein Assay Kit (ThermoFisher Scientific, Waltham, United States). Subsequently, 30 μg of the lysate was loaded onto a 10% sodium dodecyl sulfate-polyacrylamide gel and electrophoresis was run at 80 V until the sample reached the separating gel, followed by separation at 120 V. Proteins were then transferred to polyvinylidene difluoride (PVDF, Millipore, Billerica, MA, United States) membranes after electrophoresis. PVDF membranes were blocked with 5% skim milk for 1 h at room temperature, followed by overnight incubation at 4 °C with antibodies against *NRF2*, *HO-1*, *NQO-1*,

collagen I, collagen IV, and fibronectin (Proteintech, Wuhan, China). After washing with Tris-buffered saline with Tween 20 (TBST) buffer, membranes were incubated with a horseradish peroxidase-conjugated secondary antibody (Proteintech) for 2 h at room temperature, with intermittent TBST buffer washes. Protein bands were visualized using a chemiluminescent reagent (Thermo Fisher Scientific) and quantified by densitometry analysis.

Statistical analysis

Data of all the experimental results are represented as the mean \pm SD. Data analyses were conducted using a *t*-test or one-way analysis of variance (ANOVA) followed by the *post-hoc* Tukey's test to compare the differences between groups at a significance level of $P < 0.05$.

RESULTS

AC inhibits the proliferation of HG-induced HBZY-1 cells

Prior to validating the activity of AC in HG-induced cell model, we initially assessed the cytotoxic impact of various concentrations of AC (Figure 1A), within the gradient range of 0.5 μ M to 32.0 μ M on HBZY-1 cells (Figure 1B). CCK-8 results revealed that different doses of AC (ranging from 0.5 μ M to 32.0 μ M) did not exhibit significant cytotoxic effects on viability of HBZY-1 cells. Subsequently, we introduced normal glucose (5.5 mmol/L), mannitol (30.0 mmol/L), and high glucose (HG, 30.0 mmol/L) levels in the medium along with AC to examine their impact on HBZY-1 cell proliferation. As illustrated in Figure 1C-E, the addition of HG notably enhanced the proliferation of HBZY-1 cells ($P < 0.001$), while normal glucose and mannitol did not promote cell proliferation. AC at high doses (4 μ M and 8 μ M) could effectively inhibit HG-induced proliferation of HBZY-1 cells ($P < 0.01$). These data suggest the anti-proliferation effect of AC on HG-induced HBZY-1 cells.

AC reduces HG-induced inflammatory responses and oxidative stress

The impact of different concentrations of AC on HG-induced inflammatory responses and oxidative stress was examined in HBZY-1 cells. Figure 2A and B demonstrates that the mRNA levels of *IL-6*, *IL-8*, and *TNF- α* in HBZY-1 cells, as well as their contents in the supernatant, were notably elevated following HG treatment ($P < 0.001$) compared to those in control cells. Additionally, AC led to a dose-dependent decrease in the mRNA levels of *IL-6*, *IL-8*, and *TNF- α* in HG-induced cells, as well as the contents of these cytokines in the supernatants ($P < 0.01$ or $P < 0.001$). HG treatment induced significantly higher levels of ROS and MDA in HBZY-1 cells compared to the absence of HG treatment ($P < 0.001$), while SOD activity was markedly reduced post HG treatment. A gradual reduction in ROS and MDA levels, coupled with an increase in SOD activity, was observed with increasing AC concentrations in the presence of HG treatment ($P < 0.01$ or $P < 0.001$) (Figure 2C-E).

AC suppresses HG-induced fibrosis in HBZY-1 cells

The expression levels of collagen I, collagen IV, and fibronectin serve as markers for cellular fibrosis. As shown in Figure 3, results from qRT-PCR and WB analysis demonstrated that HG treatment led to significantly elevated mRNA and protein levels of collagen I, collagen IV, and fibronectin in HBZY-1 cells ($P < 0.001$) compared to the control group. Moreover, increasing AC concentrations resulted in a gradual decrease in the mRNA and protein levels of collagen I, collagen IV, and fibronectin in HG-induced HBZY-1 cells ($P < 0.01$ or $P < 0.001$). Therefore, AC suppresses HG-induced fibrosis in HBZY-1 cells.

AC regulates the HG effect by activating the NRF2/HO-1 pathway

We further observed a decrease in nuclear NRF2 protein expression and total HO-1 and NQO-1 protein levels in HBZY-1 cells following HG treatment. Conversely, AC treatment led to increased levels of nuclear NRF2, total HO-1, and NQO-1 proteins in a dose-dependent manner (Figure 4A). The requirement of NRF2 in the activity of AC was further elucidated by using the NRF2 inhibitor ML385. The combination treatment of HG + AC + ML385 reduced protein expression levels of nuclear NRF2, HO-1, and NQO-1 (Figure 4B). Moreover, the anti-inflammatory effect of AC on *IL-6*, *IL-8*, and *TNF- α* was abolished after ML385 inhibition of NRF2 activity (Figure 4C). Similar results were observed in the oxidative stress, as evidenced by the elevated ROS and MDA levels, as well as the decreased SOD activity upon ML385 treatment (Figure 4D). Besides, ML385 treatment also increased the levels of collagen I, collagen IV, and fibronectin proteins after HG + AC treatment (Figure 4E). These results suggest that AC may modulate the effects of HG by activating the NRF2/HO-1 pathway.

AC mitigates oxidative stress and fibrosis in a DN rat model

Subsequently, we evaluated the effect of AC administration on oxidative stress and fibrosis in a DN rat model. Compared with the sham group, no significant differences in the body weight, blood glucose, kidney weight/body weight ratio, serum creatinine, blood urea nitrogen, and 24-h urinary protein were observed in the AC treatment alone group. Compared to the sham group, the body weight, blood glucose, serum creatinine, blood urea nitrogen, and 24-h urinary protein were significantly elevated in the DN group. AC administration significantly reduced body weight and biochemical parameters in the DN model group, such as blood glucose, serum creatinine, blood urea nitrogen, and 24-h urinary protein levels (Figure 5A-F).

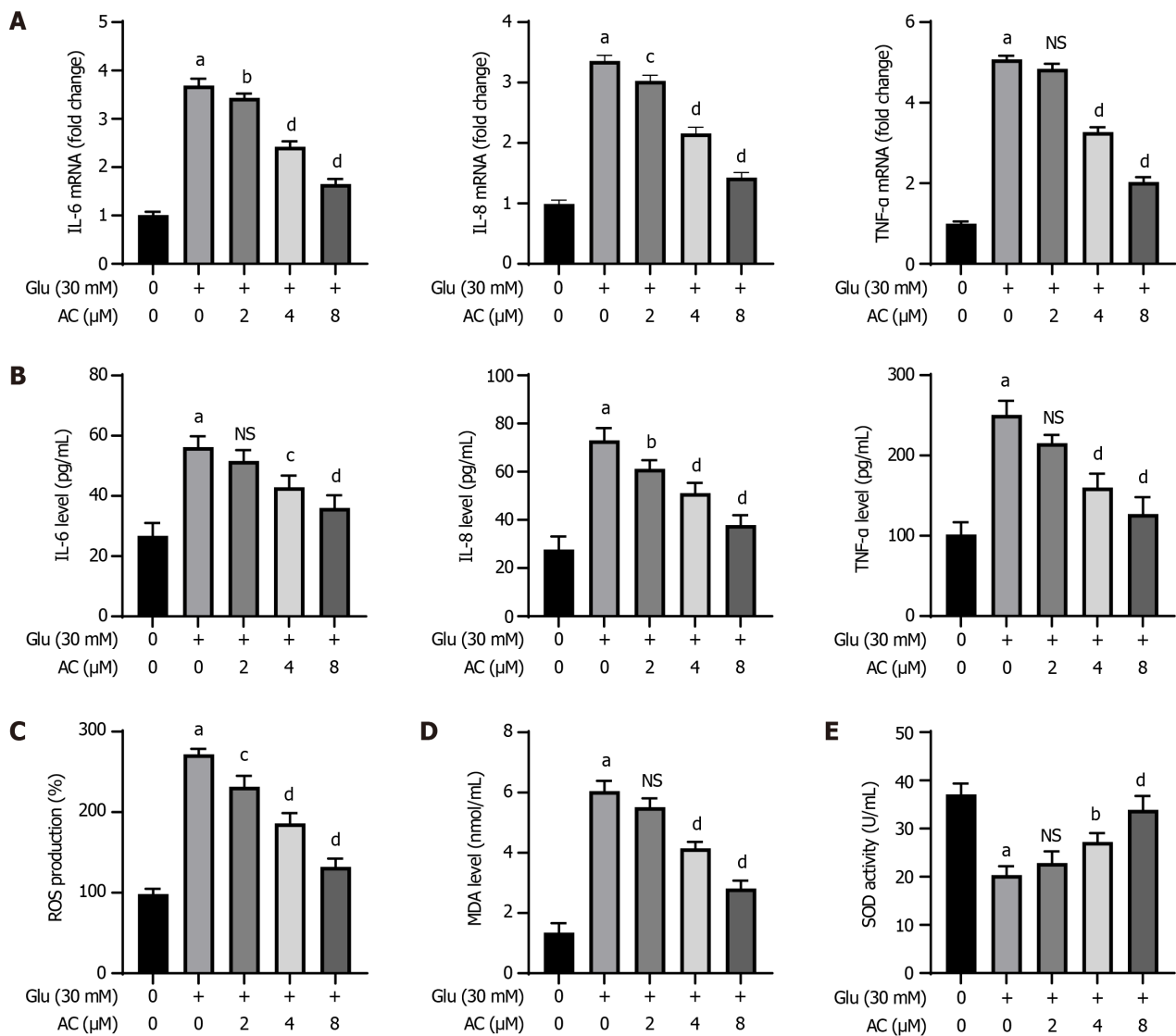


Figure 2 Effect of asiaticoside on high glucose-induced inflammatory response and oxidative stress in rat glomerular mesangial cells. A: Quantitative real-time polymerase chain reaction analysis of the mRNA levels of interleukin (IL)-6, IL-8, and tumor necrosis factor (TNF)-α in rat glomerular mesangial (HBZY-1) cells treated with asiaticoside at different concentrations (0, 2, 4, and 8 μM) and glucose (30 mmol/L); B: IL-6, IL-8, and TNF-α in the supernatant of HBZY-1 cells determined by ELISA; C-E: Reactive oxygen species, malondialdehyde, and superoxide dismutase levels in HBZY-1 cells determined by ELISA using corresponding kits. *n* = 3 experiments. ^a*P* < 0.001 vs control, ^b*P* < 0.05, ^c*P* < 0.01, and ^d*P* < 0.001 (Glu, 30 mmol/L + AC, 0 μM); not significant (*P* > 0.05) vs (Glu, 30 mmol/L + AC 0 μM). AC: Asiaticoside; Glu: Glucose; NS: Not significant.

The renal histological observations in the AC group revealed no significant changes in the renal tissues compared to those in the sham group (Figure 5G). However, HE staining showed an increase in renal inflammatory infiltration in the DN model group. Additionally, Masson’s staining indicated severe renal interstitial fibrosis in the DN model group, PAS staining showed glomerular hypertrophy and mesangial matrix dilation, and TEM imaging revealed podocyte detachment and disappearance. These pathophysiological changes in the rat model were largely mitigated with AC treatment. Besides, there were no significant differences in the levels of IL-6, IL-8, TNF-α, MDA, and SOD in the serum of rats of the AC treatment group compared to the sham group. The DN group exhibited significantly increased levels of IL-6, IL-8, TNF-α, and MDA, with a considerable decrease in SOD activity. AC treatment resulted in a significant reversal of these changes compared to the DN group, indicating that AC effectively alleviated inflammatory and oxidative stress in the DN rats (Figure 5H and I).

We further analyzed the expression levels of proteins related to fibrosis in the renal tissues. Compared to the sham group, there were no significant changes in the levels of collagen I, collagen IV, and fibronectin proteins in the renal tissues of rats of the AC treatment alone group. The DN group showed significantly higher expression levels of these fibrogenic markers, while AC administration resulted in a notable decrease in the levels of collagen I, collagen IV, and fibronectin proteins in the renal tissues of rats of the DN model group (Figure 5J). Additionally, the DN group displayed decreased levels of nuclear NRF2 and total HO-1, as well as NQO-1 proteins in the renal tissues. However, AC treatment restored the expression of nuclear NRF2 and total HO-1, as well as NQO-1 protein levels, indicating activation of the NRF2 signaling pathway by AC (Figure 5K).

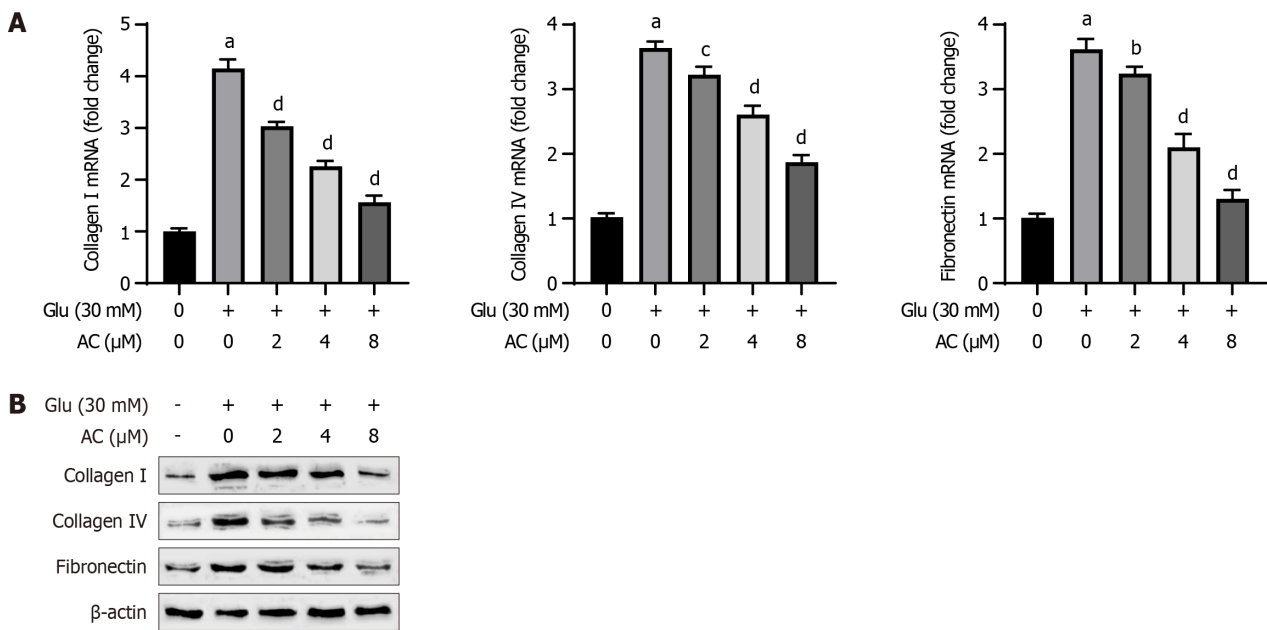


Figure 3 Effect of asiaticoside on high glucose-induced fibrosis in rat glomerular mesangial cells. A: Quantitative real-time polymerase chain reaction analysis of the mRNA levels of collagen I, collagen IV, and fibronectin in rat glomerular mesangial (HBZY-1) cells treated with asiaticoside at different concentrations (0, 2, 4, and 8 μ M) and glucose (30 mmol/L); B: Western blot analysis of the protein levels of collagen I, collagen IV, and fibronectin in HBZY-1 cells. $n = 3$ experiments. ^a $P < 0.001$ vs control; ^b $P < 0.05$, ^c $P < 0.01$, and ^d $P < 0.001$ vs Glu (30 mmol/L). AC: Asiaticoside; Glu: Glucose.

DISCUSSION

This study demonstrated that AC inhibited HG-induced proliferation, inflammatory responses, oxidative stress, and fibrosis in HBZY-1 cells, and ameliorated renal injury in a streptozotocin-induced DN rat model. AC reduced levels of inflammatory cytokines, ROS, MDA, and fibrogenic markers while increasing superoxide dismutase (SOD) activity. Notably, the renoprotective effects of AC were associated with the activation of the NRF2/HO-1 signaling pathway, suggesting that AC may have therapeutic potential for DN by targeting inflammation, oxidative stress, and fibrosis through NRF2-associated antioxidant mechanisms.

HBZY-1 cells are one of the major cell types used in the study of renal defects such as DN[17]. The abnormal proliferation of mesangial cells is increasingly recognized as potentially playing a crucial role in the pathophysiological mechanism of early DN. A previous study has indicated that HG can significantly increase the proliferation of HBZY-1 cells, leading to renal interstitial fibrosis and ultimately chronic kidney failure[18]. Building on this foundation, HBZY-1 cells were exposed to normal glucose, high mannitol, and HG in this study. The results showed that HG notably enhanced the proliferation of HBZY-1 cells, whereas glucose or mannitol had no significant impact on their proliferation. Treatment with AC inhibited the HG-induced proliferation of HBZY-1 cells in a dose-dependent manner.

Prior research has established a strong correlation between heightened cellular oxidative stress triggered by hyperglycemia and the onset as well as progression of DN[19]. This increase in ROS levels could directly result from hyperglycemia-induced oxidative stress[20]. Among the products of oxidative stress, MDA signifies the end product of lipid peroxidation caused by free radicals, with higher MDA levels indicating a more severe oxidative stress response[21]. SOD serves as a crucial antioxidant marker that facilitates the conversion of superoxide to oxygen and hydrogen peroxide[22]. The levels of MDA and SOD are utilized to gauge the degree of oxidative stress in cell and renal tissues. In this study, a notable rise in ROS and MDA levels was observed in HG-treated HBZY-1 cells and in renal tissues of DN rats. Additionally, SOD activities were significantly decreased in the HG-induced cell model and in DN rats. Treatment with AC resulted in a marked reversal of these effects on SOD and MDA levels in both HBZY-1 cells and DN rats, indicating that AC could effectively mitigate oxidative stress in DN rats and mesangial cells induced by HG.

Inflammatory responses in DN are primarily triggered by oxidative stress, leading to accelerated renal injury in rats. Tashiro *et al*[23] found high levels of pro-inflammatory factors in early-stage DN patients. Similarly, our study observed significant increases in IL-6, IL-8, and TNF- α levels in the serum of DN rats, as well as in the mRNA levels of these cytokines in HBZY-1 cells treated with HG. Treatment with AC reversed these changes, demonstrating a strong anti-inflammatory effect which can be attributed to its effect to antagonize the oxidative stress.

The main pathological characteristics of DN involve thickening of the glomerular basement membrane, dilation of the mesangium, glomerulosclerosis, and tubulointerstitial fibrosis[24]. In this study, we utilized H&E, Masson's, and PAS staining techniques to assess the pathogenic changes in the renal tissues. Treatment with AC was found to significantly mitigate pathological renal damage in rats. Collagen IV and fibronectin are commonly used as fibrosis markers in DN clinical diagnosis[25,26]. Our findings revealed a notable increase in the expression levels of collagen I, collagen IV, and fibronectin in the renal tissues of DN rats induced by STZ, indicating a significant rise in renal interstitial fibrosis in DN rats. In line with this, both mRNA and protein levels of collagen I, collagen IV, and fibronectin were markedly elevated in

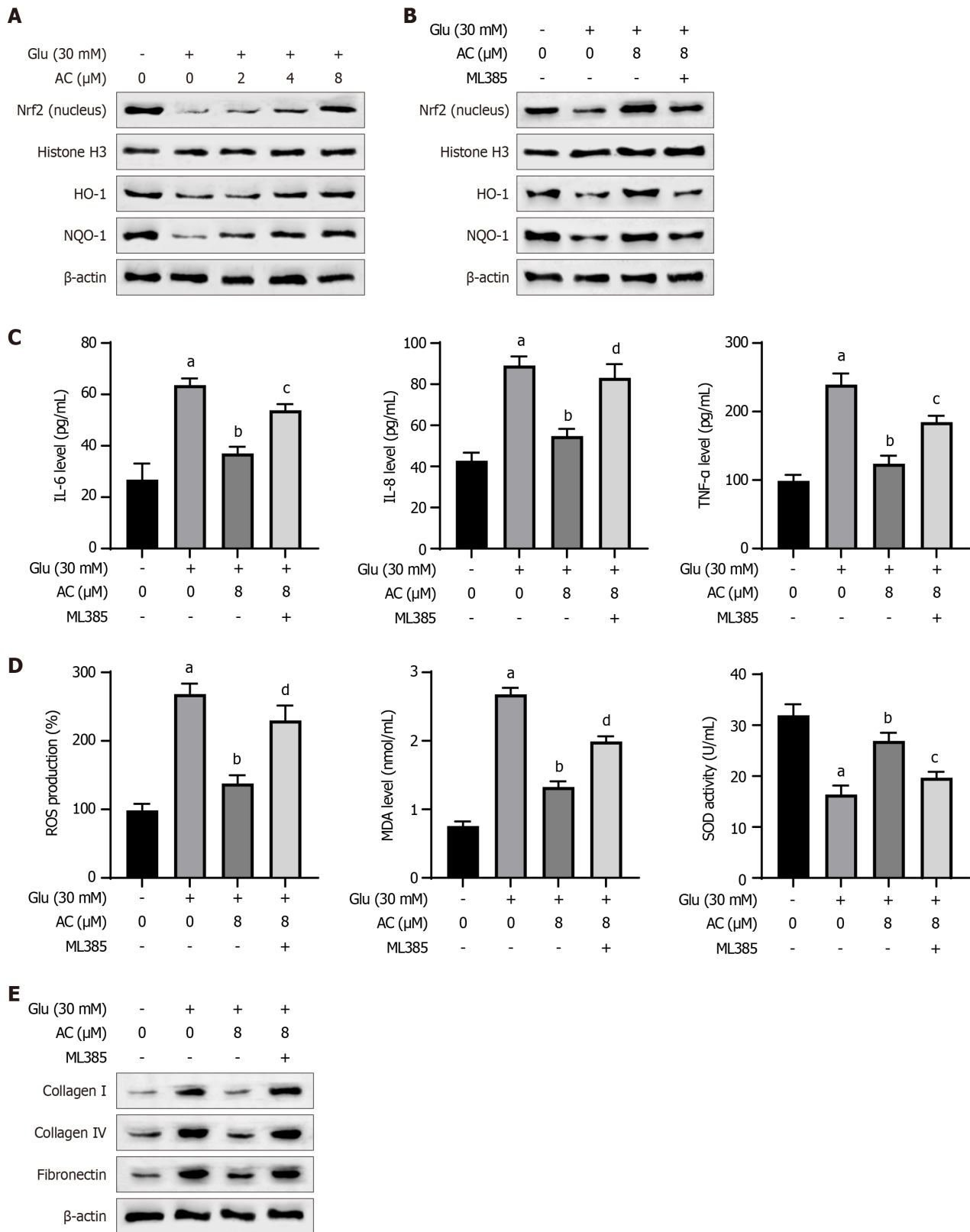
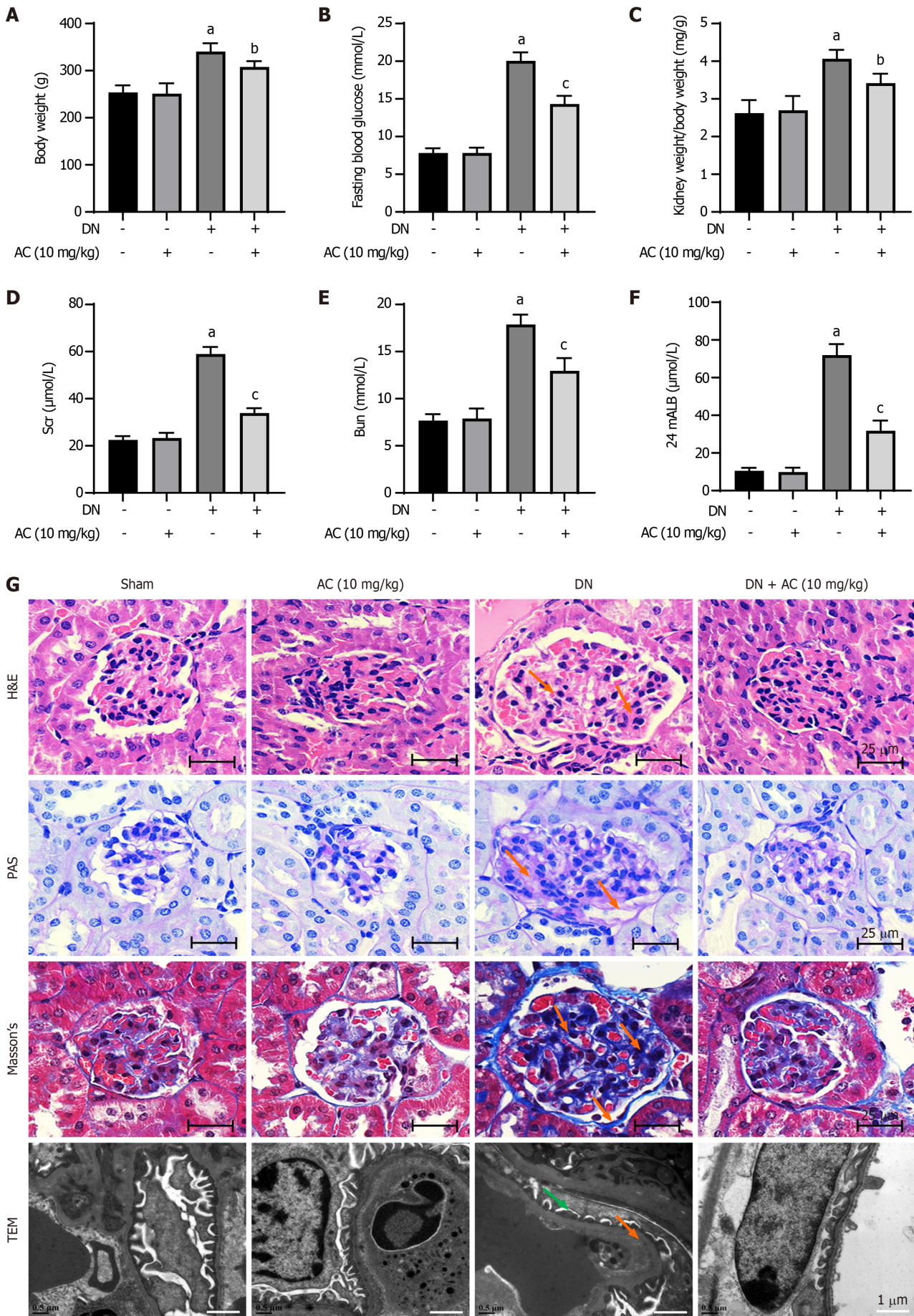


Figure 4 Asiaticoside regulates high glucose-induced effects on rat glomerular mesangial cells by activating the NRF2/ heme oxygenase-1 pathway. A: Western blot analysis of the NRF2 protein expression and total heme oxygenase-1 (HO-1) and NAD(P)H dehydrogenase (Quinone) 1 (NQO-1) protein expression in the nucleus of rat glomerular mesangial (HBZY-1) cells treated with asiaticoside (AC) at different concentrations (0, 2, 4, and 8 μ M) and glucose (30 mmol/L); B: Western blot analysis of NRF2 protein expression and total HO-1 and NQO-1 protein expression in the nucleus of HBZY-1 cells treated with AC (8 μ M), glucose (30 mmol/L), and ML385 (NRF2 inhibitor, 5 μ M); C: Interleukin (IL)-6, IL-8, and tumor necrosis factor- α levels in the supernatant of HBZY-1 cells; D: Reactive oxygen species, malondialdehyde, and superoxide dismutase in HBZY-1 cells; E: Western blot analysis of the expression levels of collagen I, collagen IV, fibronectin, and β -actin in HBZY-1 cells. $n = 3$ experiments. ^a $P < 0.001$ vs control, ^b $P < 0.001$ vs Glu (30 mmol/L), ^c $P < 0.01$, and ^d $P < 0.001$ vs Glu (30 mmol/L) + AC (8 μ M). AC: Asiaticoside; Glu: Glucose.



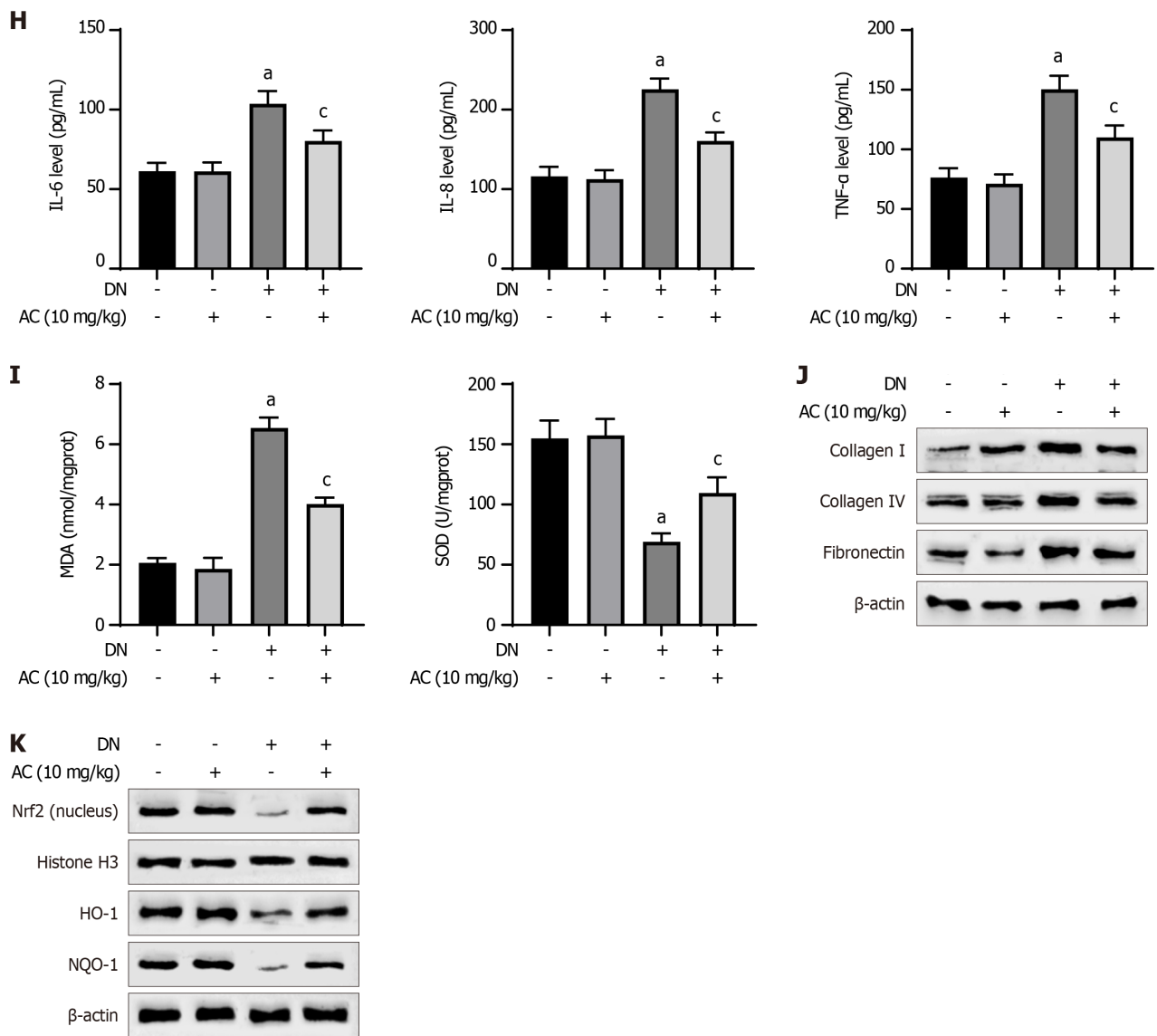


Figure 5 Asiaticoside attenuates oxidative stress and fibrosis in a diabetic nephropathy rat model. A-F: Graphical summary of the changes in body weight, blood glucose, kidney weight/body weight ratio, serum creatinine, blood urea nitrogen, and 24-h urine protein in control, diabetic nephropathy (DN) model, asiaticoside (AC) drug, and DN + AC groups; G: Results of hematoxylin and eosin (scale bar: 25 μ m, orange arrows indicate mesangial hyperplasia), Masson's (scale bar: 25 μ m, orange arrows mark collagen fiber deposition), and Periodic acid-Schiff staining (scale bar: 25 μ m, orange arrows indicate glycogen deposition), as well as TEM (scale bar: 1 μ m, orange arrow shows uniform thickening of the basement membrane, and green arrow indicates loss of the podocyte foot process); H and I: Graphical summary of (H) the contents of interleukin (IL)-6, IL-8, and tumor necrosis factor (TNF)- α , and (I) the contents of malondialdehyde and superoxide dismutase in rat serum of each experimental group; J: Western blot analysis of the protein expression of collagen I, collagen IV, and fibronectin; K: Protein expression of nuclear NRF2 and total heme oxygenase-1, as well as NAD(P)H dehydrogenase (Quinone) 1, in renal tissues. $n = 6$ animals in each group. ^a $P < 0.001$ vs Sham, ^b $P < 0.05$, and ^c $P < 0.001$ vs diabetic nephropathy. DN: Diabetic nephropathy; AC: Asiaticoside; PAS: Periodic acid-Schiff; TEM: Transmission electron microscopy; HO-1: Heme oxygenase-1; NQO-1: NAD(P)H dehydrogenase (Quinone) 1; IL: Interleukin; TNF: Tumor necrosis factor; H&E: Hematoxylin and eosin.

HG-treated HBZY-1 cells. Treatment with AC effectively suppressed these changes, suggesting that AC could attenuate renal injury in diabetic rats by inhibiting renal interstitial fibrosis.

The NRF2/HO-1 signaling pathway plays a significant role in counteracting oxidative stress, and recent research has highlighted that enhancing NRF2/HO-1 signaling can mitigate renal injury in diabetic rats[27]. In response to oxidative stress, NRF2 translocates to the nucleus and triggers the expression of HO-1 and NQO-1. We observed a significant activation of nuclear NRF2 expression, total HO-1, and NQO-1 protein in kidney tissue of DN rats and HBZY-1 cells following AC treatment. These results suggest that the beneficial effects of AC on inflammation, oxidative stress, and renal fibrosis may be linked to the activation of the NRF2/HO-1 pathway. Furthermore, by using the NRF2 inhibitor ML385, the protective effect of AC on inflammatory, oxidative stress, and fibrogenic features in HBZY-1 cells was suppressed. Overall, these findings support the notion that the anti-inflammatory, anti-oxidative, and anti-fibrotic properties of AC are closely associated with the activation of the NRF2/HO-1 signaling pathway.

While this study provides valuable insights into the therapeutic potential of AC for DN, certain limitations should be acknowledged. First, the STZ-induced diabetes model used in this study may not fully recapitulate the complex pathophysiology of human DN, which often develops gradually over years in the context of chronic hyperglycemia and

metabolic dysregulation. The effect of AC should be further evaluated in genetically modified animal models. Additionally, the assessment of renal fibrosis in this study relied primarily on the evaluation of fibrogenic markers (collagen I, collagen IV, and fibronectin) and standard histological stains (Masson's trichrome and PAS). The incorporation of Picrosirius red staining, which specifically stains collagen fibrils and facilitates quantitative analysis of fibrosis, could have provided more comprehensive and quantitative insights into the extent of renal fibrosis and the mitigating effects of AC. Future studies are also warranted to elucidate how AC activates NRF2 to antagonize oxidative and inflammatory stress in DN models.

CONCLUSION

In summary, our study has demonstrated that AC could effectively ameliorate renal damages in a rat model of DN by attenuating oxidative stress, inflammatory responses, and renal fibrosis through activating the NRF2 pathway. These findings suggest that AC may be employed as a protective agent for ameliorating DN progression.

FOOTNOTES

Author contributions: Zhuang LG and Ge XX participated in literature search, study design, and manuscript writing and critical revision; Zhang R, Jin GX, Pei XY, and Wang Q participated in data collection, analysis, and interpretation; and all authors read and approved the final manuscript.

Supported by the General Project of Anhui Provincial Health and Construction Commission, No. AHWJ2022b056.

Institutional animal care and use committee statement: This animal study was reviewed and approved by the Ethics Committee of Bengbu Medical College (approval No. 2022-117).

Conflict-of-interest statement: Lan-Gen Zhuang has received research funding from the Natural Science Research Project of Anhui Educational Committee and the General project of Anhui Provincial Health and Construction Commission. Other authors declare that there are no conflicts of interest to disclose for this article.

Data sharing statement: The datasets used or/and analyzed during the current study are available from the corresponding author upon email request.

ARRIVE guidelines statement: The authors have read the ARRIVE guidelines, and the manuscript was prepared and revised according to the ARRIVE guidelines.

Open-Access: This article is an open-access article that was selected by an in-house editor and fully peer-reviewed by external reviewers. It is distributed in accordance with the Creative Commons Attribution NonCommercial (CC BY-NC 4.0) license, which permits others to distribute, remix, adapt, build upon this work non-commercially, and license their derivative works on different terms, provided the original work is properly cited and the use is non-commercial. See: <https://creativecommons.org/licenses/by-nc/4.0/>

Country of origin: China

ORCID number: Xiao-Xu Ge [0009-0002-3322-3959](https://orcid.org/0009-0002-3322-3959).

S-Editor: Chen YL

L-Editor: Wang TQ

P-Editor: Zheng XM

REFERENCES

- 1 **Anders HJ**, Huber TB, Isermann B, Schiffer M. CKD in diabetes: diabetic kidney disease *versus* nondiabetic kidney disease. *Nat Rev Nephrol* 2018; **14**: 361-377 [PMID: [29654297](https://pubmed.ncbi.nlm.nih.gov/29654297/) DOI: [10.1038/s41581-018-0001-y](https://doi.org/10.1038/s41581-018-0001-y)]
- 2 **Xiang E**, Han B, Zhang Q, Rao W, Wang Z, Chang C, Zhang Y, Tu C, Li C, Wu D. Human umbilical cord-derived mesenchymal stem cells prevent the progression of early diabetic nephropathy through inhibiting inflammation and fibrosis. *Stem Cell Res Ther* 2020; **11**: 336 [PMID: [32746936](https://pubmed.ncbi.nlm.nih.gov/32746936/) DOI: [10.1186/s13287-020-01852-y](https://doi.org/10.1186/s13287-020-01852-y)]
- 3 **Tang G**, Li S, Zhang C, Chen H, Wang N, Feng Y. Clinical efficacies, underlying mechanisms and molecular targets of Chinese medicines for diabetic nephropathy treatment and management. *Acta Pharm Sin B* 2021; **11**: 2749-2767 [PMID: [34589395](https://pubmed.ncbi.nlm.nih.gov/34589395/) DOI: [10.1016/j.apsb.2020.12.020](https://doi.org/10.1016/j.apsb.2020.12.020)]
- 4 **Hadjadj S**, Cariou B, Fumeron F, Gand E, Charpentier G, Roussel R, Kasmi AA, Gautier JF, Mohammedi K, Gourdy P, Saulnier PJ, Feigerlova E, Marre M; French JDRF Diabetic Nephropathy Collaborative Research Initiative (search for genes determining time to onset of ESRD in T1D patients with proteinuria) and the SURDIAGENE and DIABHYCAR study groups. Death, end-stage renal disease and renal function decline in patients with diabetic nephropathy in French cohorts of type 1 and type 2 diabetes. *Diabetologia* 2016; **59**: 208-216 [PMID: [26486355](https://pubmed.ncbi.nlm.nih.gov/26486355/) DOI: [10.1007/s00125-015-3785-3](https://doi.org/10.1007/s00125-015-3785-3)]

- 5 **Martínez-Castelao A**, Navarro-González JF, Górriz JL, de Alvaro F. The Concept and the Epidemiology of Diabetic Nephropathy Have Changed in Recent Years. *J Clin Med* 2015; **4**: 1207-1216 [PMID: 26239554 DOI: 10.3390/jcm4061207]
- 6 **Mathers CD**, Loncar D. Projections of global mortality and burden of disease from 2002 to 2030. *PLoS Med* 2006; **3**: e442 [PMID: 17132052 DOI: 10.1371/journal.pmed.0030442]
- 7 **Rayego-Mateos S**, Morgado-Pascual JL, Opazo-Ríos L, Guerrero-Hue M, García-Caballero C, Vázquez-Carballo C, Mas S, Sanz AB, Herencia C, Mezzano S, Gómez-Guerrero C, Moreno JA, Egido J. Pathogenic Pathways and Therapeutic Approaches Targeting Inflammation in Diabetic Nephropathy. *Int J Mol Sci* 2020; **21** [PMID: 32471207 DOI: 10.3390/ijms21113798]
- 8 **Kanwar YS**, Sun L, Xie P, Liu FY, Chen S. A glimpse of various pathogenetic mechanisms of diabetic nephropathy. *Annu Rev Pathol* 2011; **6**: 395-423 [PMID: 21261520 DOI: 10.1146/annurev.pathol.4.110807.092150]
- 9 **Vermot A**, Petit-Härtlein I, Smith SME, Fieschi F. NADPH Oxidases (NOX): An Overview from Discovery, Molecular Mechanisms to Physiology and Pathology. *Antioxidants (Basel)* 2021; **10** [PMID: 34205998 DOI: 10.3390/antiox10060890]
- 10 **Xing L**, Guo H, Meng S, Zhu B, Fang J, Huang J, Chen J, Wang Y, Wang L, Yao X, Wang H. Klotho ameliorates diabetic nephropathy by activating Nrf2 signaling pathway in podocytes. *Biochem Biophys Res Commun* 2021; **534**: 450-456 [PMID: 33256980 DOI: 10.1016/j.bbrc.2020.11.061]
- 11 **Ruiz S**, Pergola PE, Zager RA, Vaziri ND. Targeting the transcription factor Nrf2 to ameliorate oxidative stress and inflammation in chronic kidney disease. *Kidney Int* 2013; **83**: 1029-1041 [PMID: 23325084 DOI: 10.1038/ki.2012.439]
- 12 **Jiang JZ**, Ye J, Jin GY, Piao HM, Cui H, Zheng MY, Yang JS, Che N, Choi YH, Li LC, Yan GH. Asiaticoside Mitigates the Allergic Inflammation by Abrogating the Degranulation of Mast Cells. *J Agric Food Chem* 2017; **65**: 8128-8135 [PMID: 28891650 DOI: 10.1021/acs.jafc.7b01590]
- 13 **Wu X**, Bian D, Dou Y, Gong Z, Tan Q, Xia Y, Dai Y. Asiaticoside hinders the invasive growth of keloid fibroblasts through inhibition of the GDF-9/MAPK/Smad pathway. *J Biochem Mol Toxicol* 2017; **31** [PMID: 28346732 DOI: 10.1002/jbt.21922]
- 14 **Xing Y**, Ji Q, Li X, Ming J, Zhang N, Zha D, Lin Y. Asiaticoside protects cochlear hair cells from high glucose-induced oxidative stress via suppressing AGEs/RAGE/NF-κB pathway. *Biomed Pharmacother* 2017; **86**: 531-536 [PMID: 28024288 DOI: 10.1016/j.biopha.2016.12.025]
- 15 **Zhao J**, Shi J, Shan Y, Yu M, Zhu X, Zhu Y, Liu L, Sheng M. Asiaticoside inhibits TGF-β1-induced mesothelial-mesenchymal transition and oxidative stress via the Nrf2/HO-1 signaling pathway in the human peritoneal mesothelial cell line HMrSV5. *Cell Mol Biol Lett* 2020; **25**: 33 [PMID: 32514269 DOI: 10.1186/s11658-020-00226-9]
- 16 **Liu Y**, Deng J, Fan D. Ginsenoside Rk3 ameliorates high-fat-diet/streptozocin induced type 2 diabetes mellitus in mice via the AMPK/Akt signaling pathway. *Food Funct.* 2019; **10**: 2538-2551 [PMID: 30993294 DOI: 10.1039/c9fo00095j]
- 17 **Zhu X**, Shi J, Li H. Liquiritigenin attenuates high glucose-induced mesangial matrix accumulation, oxidative stress, and inflammation by suppression of the NF-κB and NLRP3 inflammasome pathways. *Biomed Pharmacother* 2018; **106**: 976-982 [PMID: 30119269 DOI: 10.1016/j.biopha.2018.07.045]
- 18 **Kanwar YS**, Wada J, Sun L, Xie P, Wallner EI, Chen S, Chugh S, Danesh FR. Diabetic nephropathy: mechanisms of renal disease progression. *Exp Biol Med (Maywood)* 2008; **233**: 4-11 [PMID: 18156300 DOI: 10.3181/0705-MR-134]
- 19 **Pennathur S**, Heinecke JW. Mechanisms for oxidative stress in diabetic cardiovascular disease. *Antioxid Redox Signal* 2007; **9**: 955-969 [PMID: 17508917 DOI: 10.1089/ars.2007.1595]
- 20 **Lu Q**, Zhai Y, Cheng Q, Liu Y, Gao X, Zhang T, Wei Y, Zhang F, Yin X. The Akt-FoxO3a-manganese superoxide dismutase pathway is involved in the regulation of oxidative stress in diabetic nephropathy. *Exp Physiol* 2013; **98**: 934-945 [PMID: 23159718 DOI: 10.1113/expphysiol.2012.068361]
- 21 **Szeto HH**. Mitochondria-targeted peptide antioxidants: novel neuroprotective agents. *AAPS J* 2006; **8**: E521-E531 [PMID: 17025271 DOI: 10.1208/aapsj080362]
- 22 **Navarro-González JF**, Mora-Fernández C. The role of inflammatory cytokines in diabetic nephropathy. *J Am Soc Nephrol* 2008; **19**: 433-442 [PMID: 18256353 DOI: 10.1681/ASN.2007091048]
- 23 **Tashiro K**, Koyanagi I, Saitoh A, Shimizu A, Shike T, Ishiguro C, Koizumi M, Funabiki K, Horikoshi S, Shirato I, Tomino Y. Urinary levels of monocyte chemoattractant protein-1 (MCP-1) and interleukin-8 (IL-8), and renal injuries in patients with type 2 diabetic nephropathy. *J Clin Lab Anal* 2002; **16**: 1-4 [PMID: 11835523 DOI: 10.1002/jcla.2057]
- 24 **Zheng ZC**, Zhu W, Lei L, Liu XQ, Wu YG. Wogonin Ameliorates Renal Inflammation and Fibrosis by Inhibiting NF-κB and TGF-β1/Smad3 Signaling Pathways in Diabetic Nephropathy. *Drug Des Devel Ther* 2020; **14**: 4135-4148 [PMID: 33116403 DOI: 10.2147/DDDT.S274256]
- 25 **Wang JY**, Yin XX, Wu YM, Tang DQ, Gao YY, Wan MR, Hou XY, Zhang B. Ginkgo biloba extract suppresses hypertrophy and extracellular matrix accumulation in rat mesangial cells. *Acta Pharmacol Sin* 2006; **27**: 1222-1230 [PMID: 16923344 DOI: 10.1111/j.1745-7254.2006.00360.x]
- 26 **Xu W**, Shao X, Tian L, Gu L, Zhang M, Wang Q, Wu B, Wang L, Yao J, Xu X, Mou S, Ni Z. Astragaloside IV ameliorates renal fibrosis via the inhibition of mitogen-activated protein kinases and antiapoptosis *in vivo* and *in vitro*. *J Pharmacol Exp Ther* 2014; **350**: 552-562 [PMID: 24951279 DOI: 10.1124/jpet.114.214205]
- 27 **Feng X**, Zhao J, Ding J, Shen X, Zhou J, Xu Z. LncRNA Blnc1 expression and its effect on renal fibrosis in diabetic nephropathy. *Am J Transl Res* 2019; **11**: 5664-5672 [PMID: 31632538]



Published by **Baishideng Publishing Group Inc**
7041 Koll Center Parkway, Suite 160, Pleasanton, CA 94566, USA
Telephone: +1-925-3991568
E-mail: office@baishideng.com
Help Desk: <https://www.f6publishing.com/helpdesk>
<https://www.wjgnet.com>

